Improving EMI shielding of graphene oxide (GNO) coated glass-fiber-GNO-MA-grafted Polypropylene composites, and Nylon-1D, 2D composite foams.

Supplementary

1. Schemes

Nylon based composites preparation

2.1.5. *Preparation of nylon-graphene-copper nanoplate composite (NGCu)*

The graphene and Cu nanoplate were added together into a Teflon bottle and shake well by hand and then filled into the mold which already consist of 40 g of nylon-carbon fiber composition. Finally, the composition was pressed for 5 min and heated at 290℃ for 2 h. The cooled composite used for further analysis.

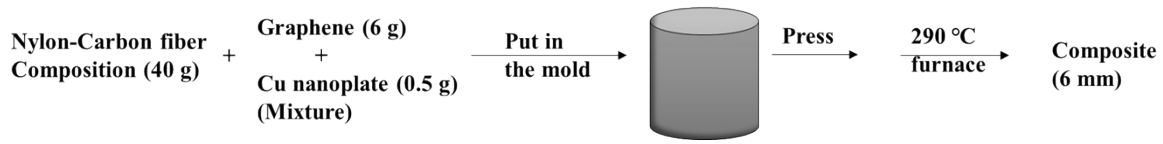

Scheme S1. Preparation of NGCu

2.1.6. Preparation of nylon-graphene-CNT NGT

The graphene and CNT were added together into a Teflon bottle and shake well by hand and then filled into the mold which already consist of 40 g of nylon-carbon fiber composition. Finally, the composition was pressed for 5 min and heated at 290℃ for 2 h. The cooled composite used for further analysis.

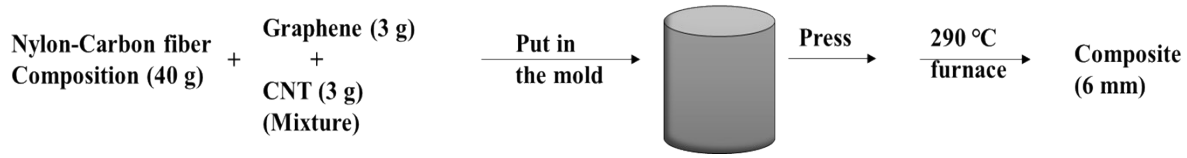

Scheme S2. Preparation of NGT

2.1.7. Preparation of nylon-CF-graphene-CNT composite (NFGT).

The graphene and Cu nanoplate were added together into a Teflon bottle. The 40 g of nylon-carbon fiber composition, and Graphene-CNT mixture were equally divided into three portions. Then one portion of nylon-carbon fiber composition, and Graphene-CNT mixture was filled into the mold and then placed one layer of carbon fabric. This process was repeated one more time and ~2 mm gab was maintained between each carbon fabric. Finally, the composition was pressed for 5 min and heated at 290℃ for 2 h. The cooled composite used for further analysis.

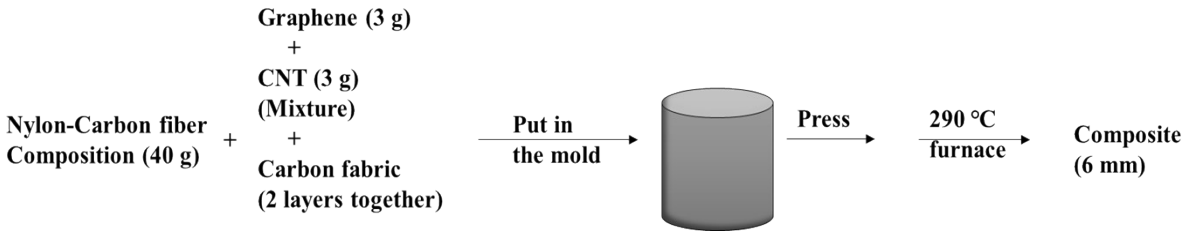

Scheme S3. Preparation of NFGT

2.1.8. Preparation of Nylon-CF-cobalt nanoplate coated CF-CNT composite (NFCoT)

The 40 g of nylon-carbon fiber composition, and Graphene were equally divided into four portions. Then one portion of nylon-carbon fiber composition, and Graphene was filled into the mold and then placed one layer of carbon fabric. This process was repeated two more time and ~1 mm gab was maintained between each carbon fabric (Co coated carbon fabric placed between 2 carbon fabric). Finally, the composition was pressed for 5 min and heated at 290°C for 2 h. The cooled composite used for further analysis.

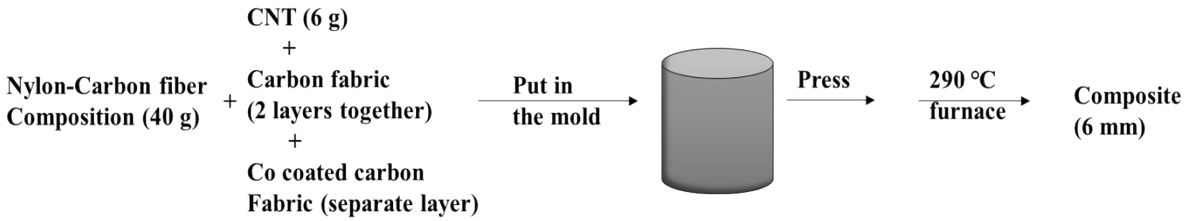

Scheme S4. Preparation of NFCoT

2.2.1. Surface modification of glass fiber (GF)

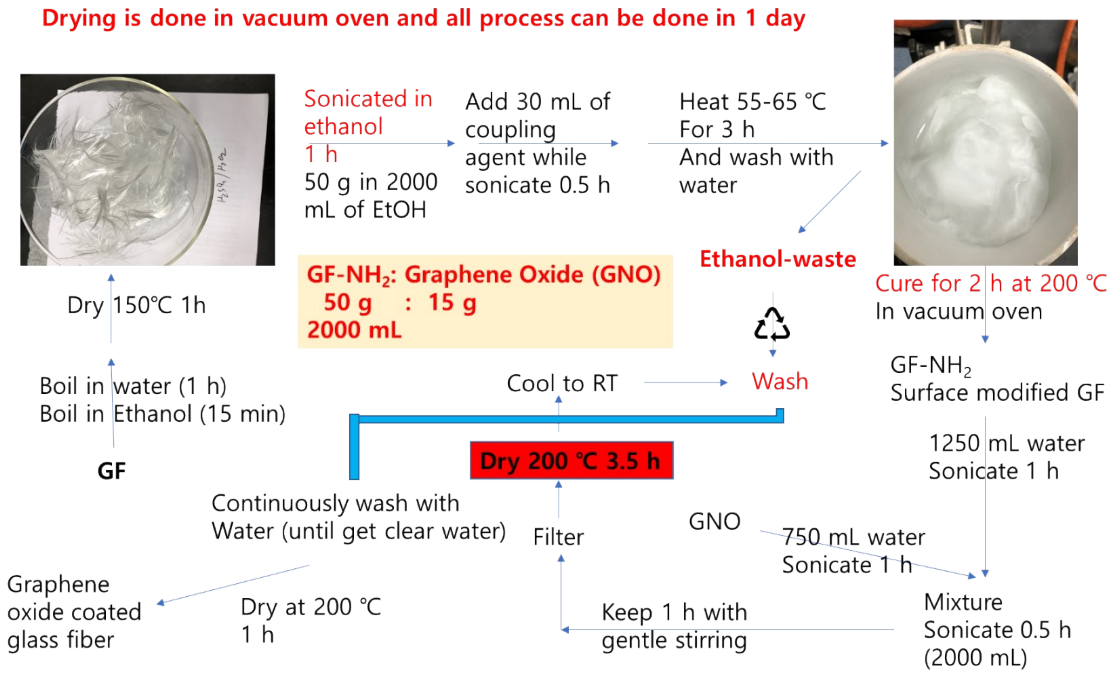

Scheme S5. The schematic representation of GF-NH_2 synthesis

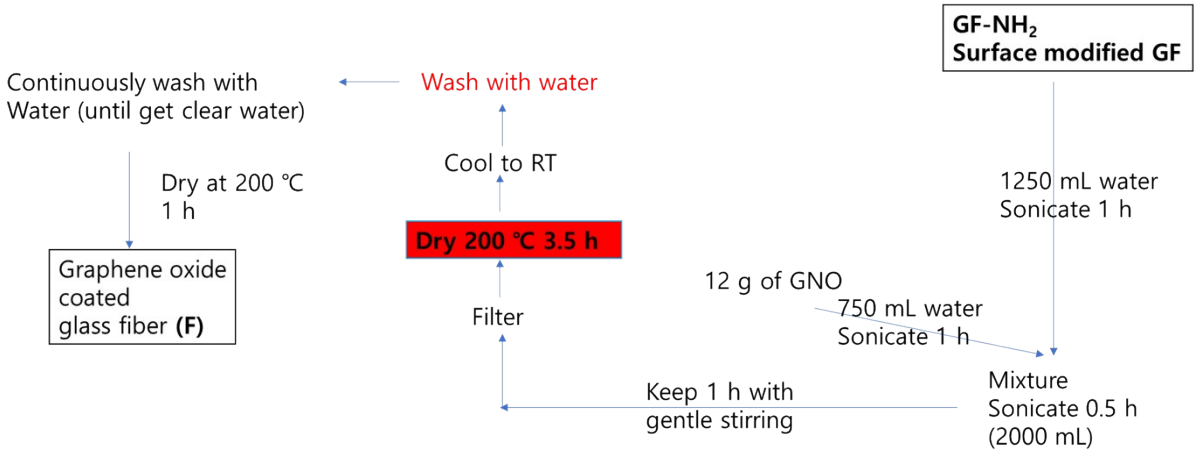

Scheme S6. The schematic representation of GNO coated GF synthesis.

2.2.4.2. GGF-maleic anhydride grafted polypropylene graphene oxide composite (GFGMAPP) (model 1)

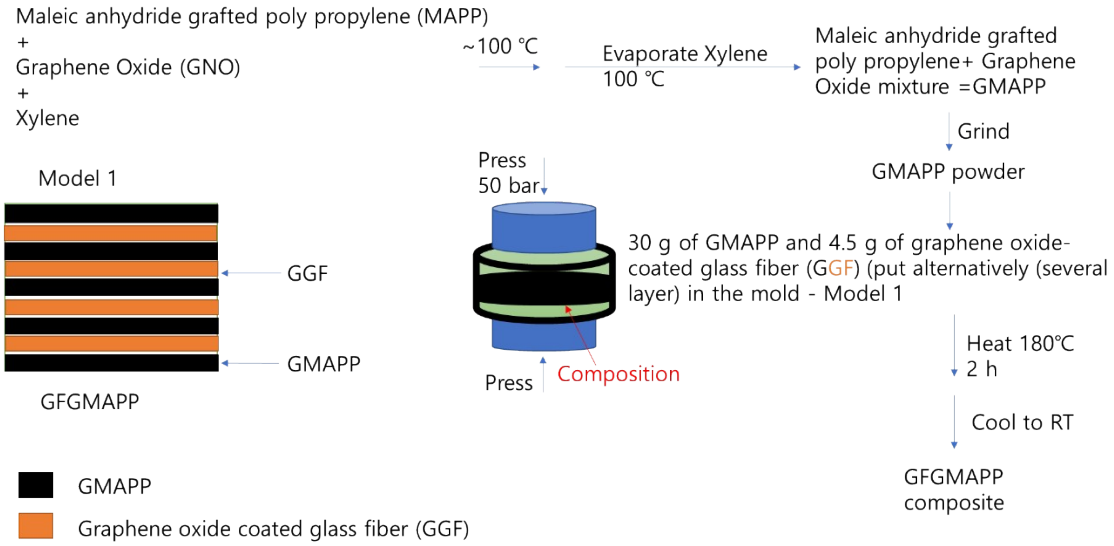

Scheme S7. Schematic representation of model 1.

2.2.4.3. GGF-CF-maleic anhydride grafted polypropylene graphene oxide composite (GFCFGMAPP) (model 2)

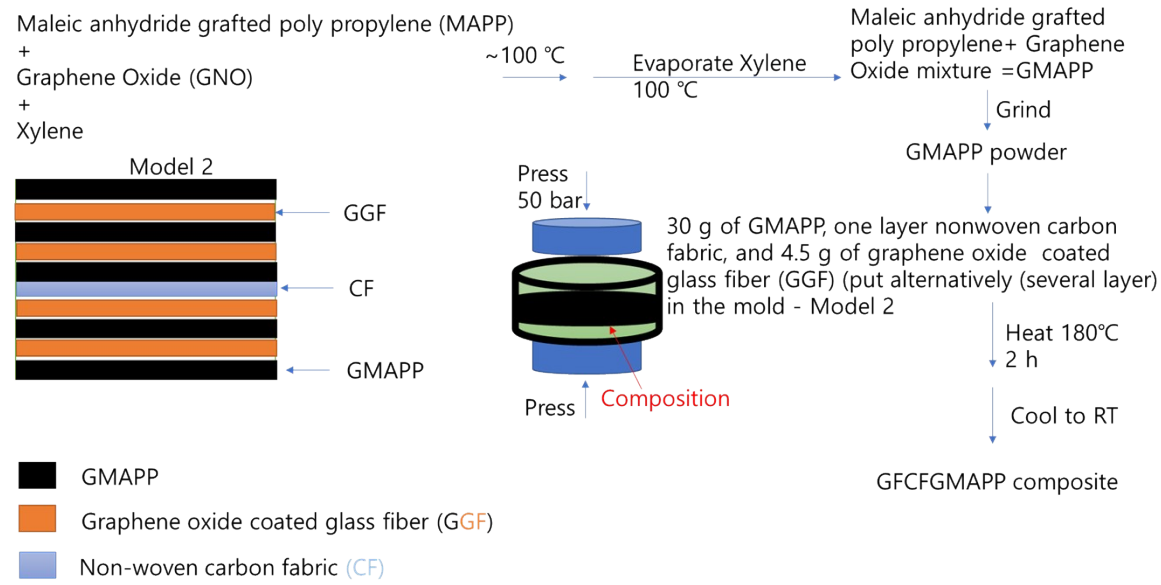

Scheme S8. Schematic representation of model 2.

2.2.4.4. GGF-CF-Fe-maleic anhydride grafted polypropylene graphene oxide nanoplate composite (GFCFFeGMAPP) (model 3)

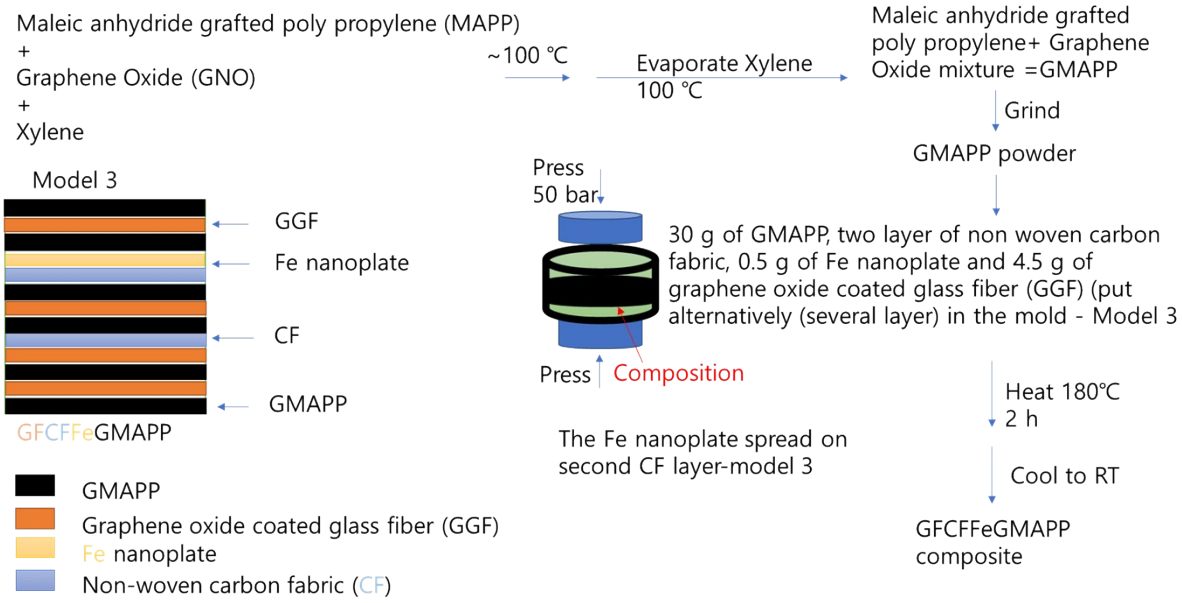

Scheme S9. Schematic representation of model 3.

2. Figure

Mold structure

The mold has been designed by us for the composite preparation shown in figure 3a-b. The inner diameter of the mold 8 cm and height is 6 cm. The metal block A set in one side and the composite was filled via other-side and finally pressed. The metal ring D is used to remove the A after the heating process.

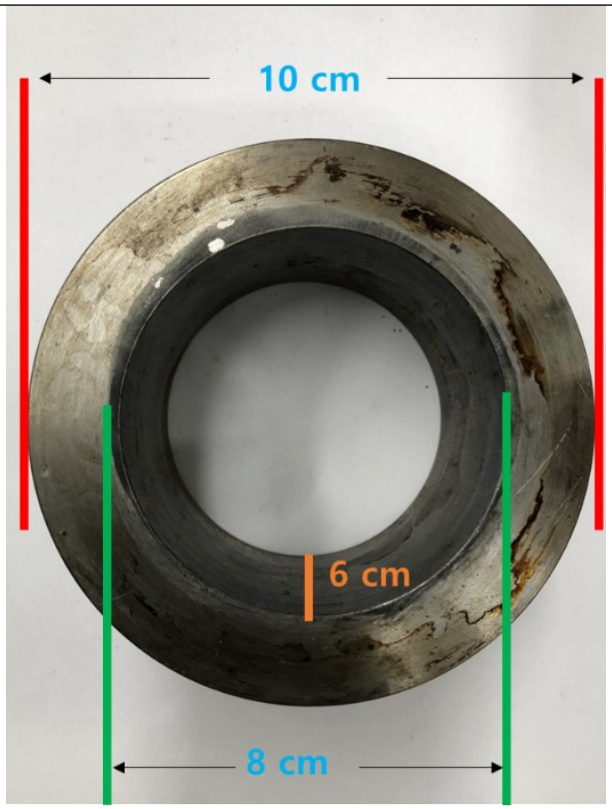

(a)

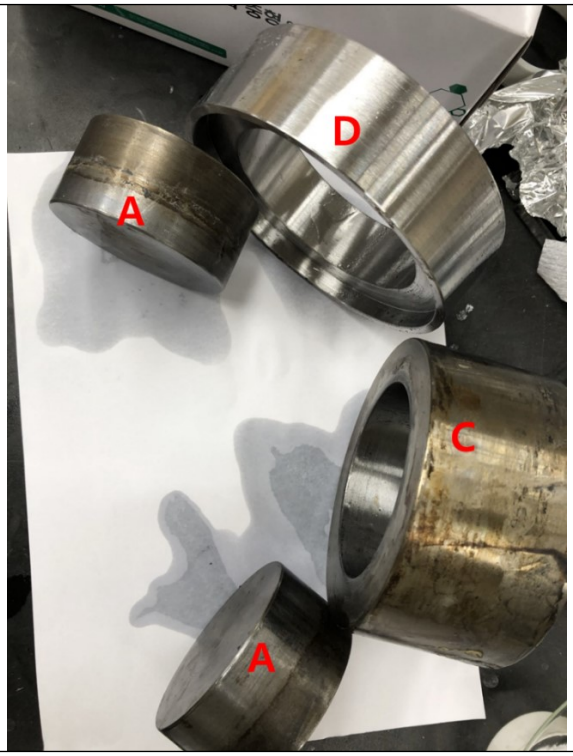

(b)

Figure S1. The structure of the mold used

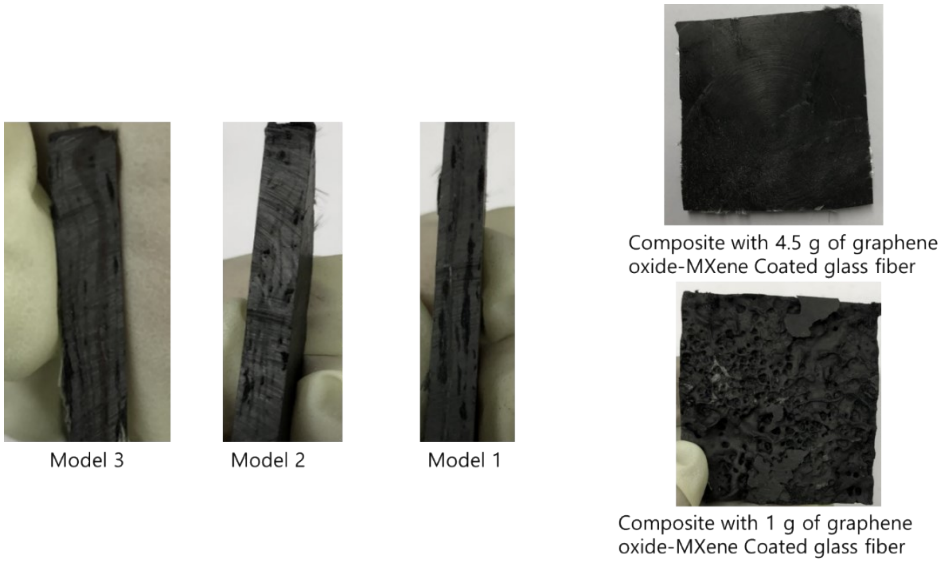

Figure S2. The photography of the composites.

3.1.3. XPS analysis

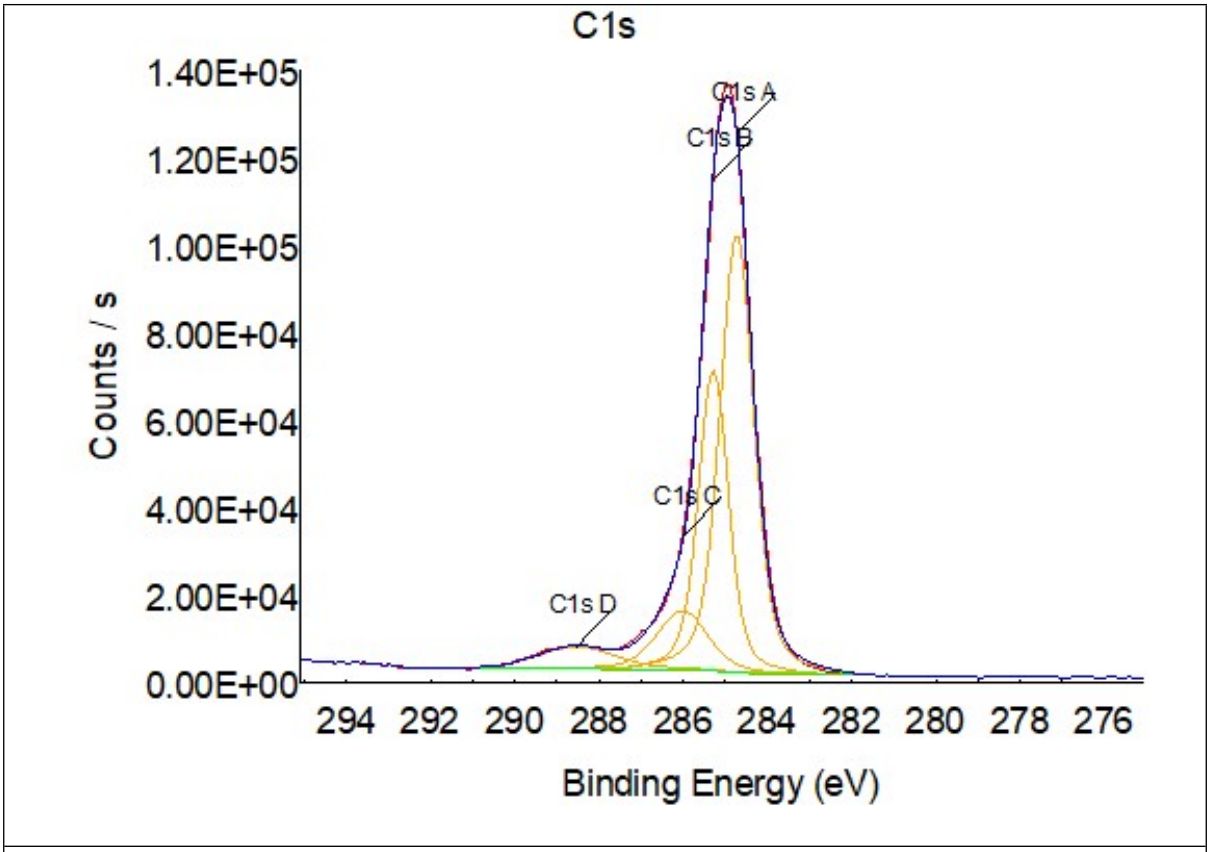

C1s GFGMAPP

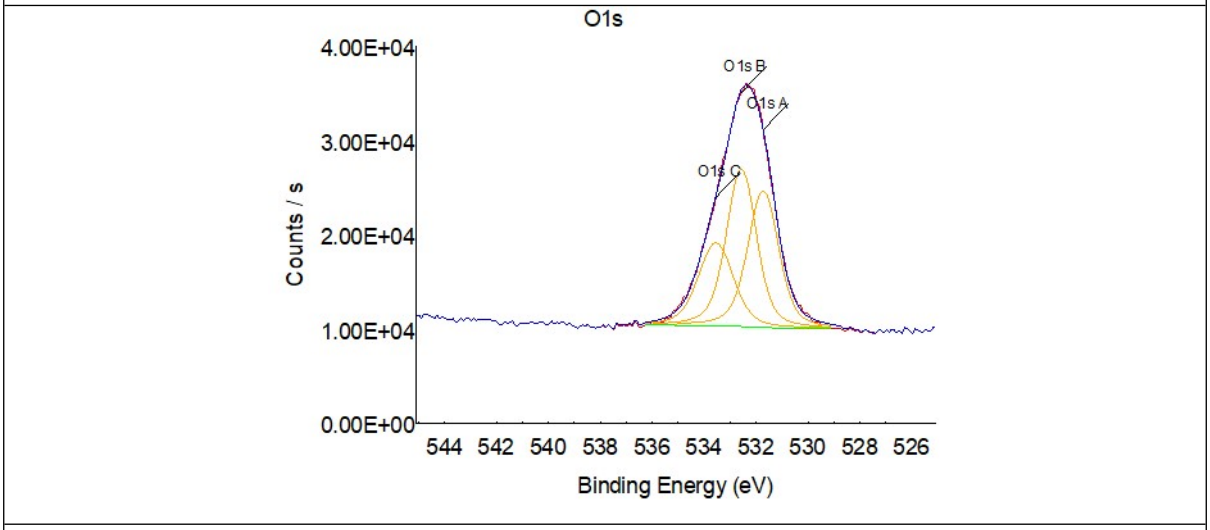

O1s GFGMAPP

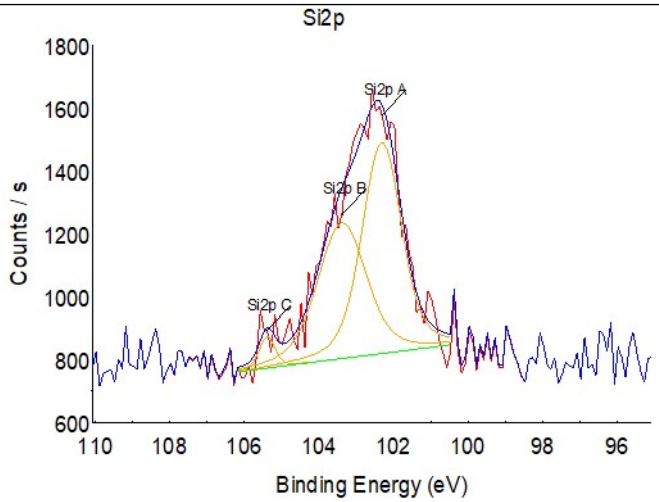

Si2p GFGMAPP

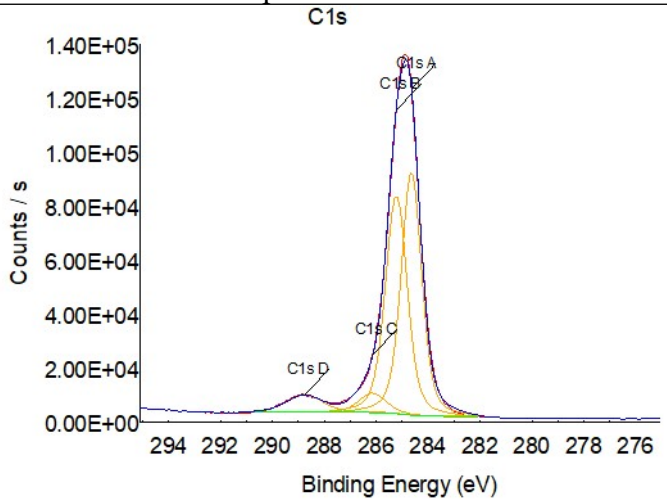

C1s GFCFGMAPP

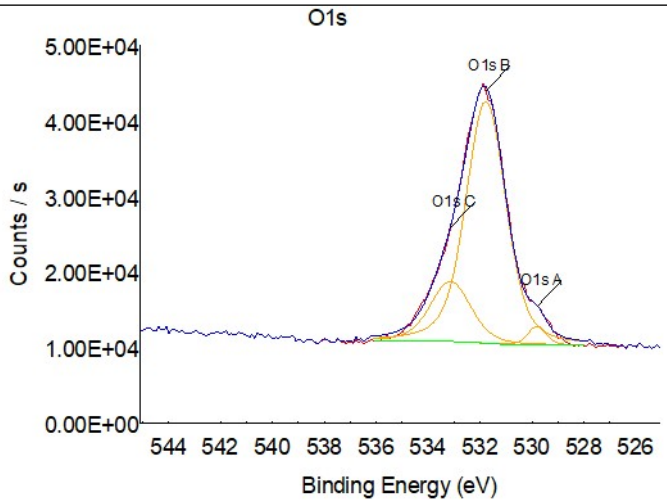

O1s GFCFGMAPP

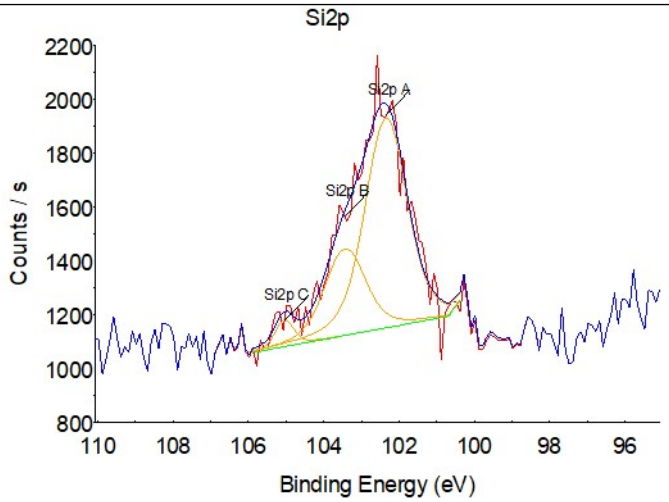

Si2p GFCFGMAPP

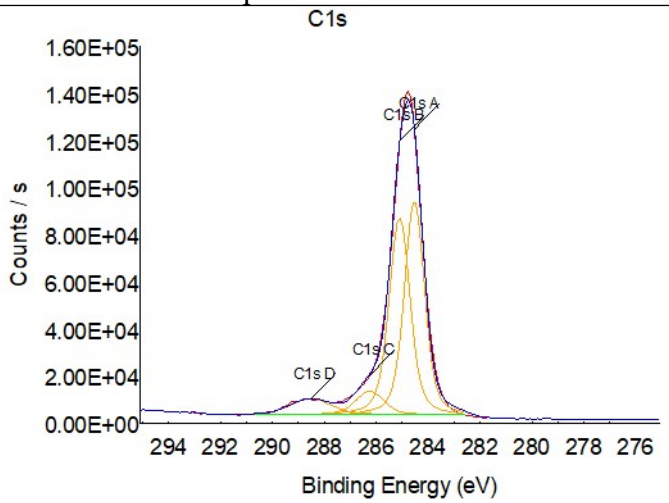

C1s GFCFFeGMAPP

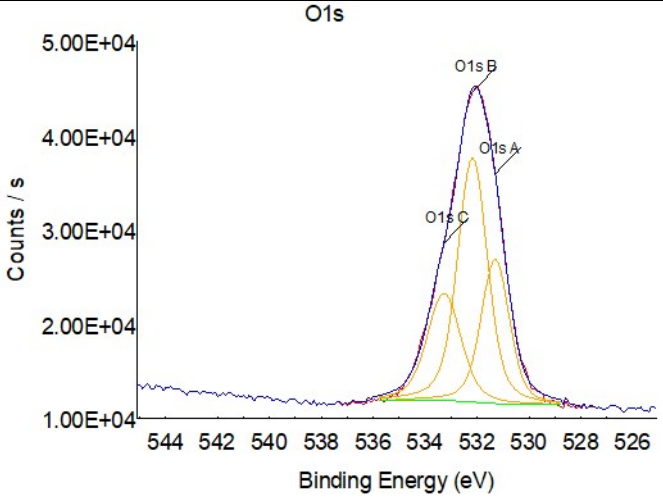

O1s GFCFFeGMAPP

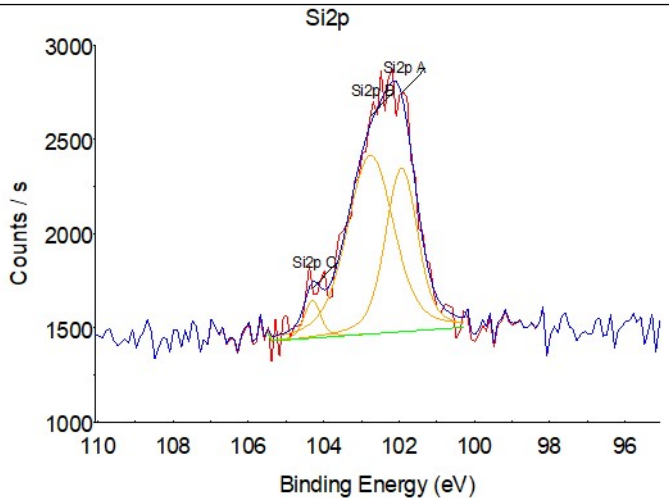

Si2p GFCFFeGMAPP

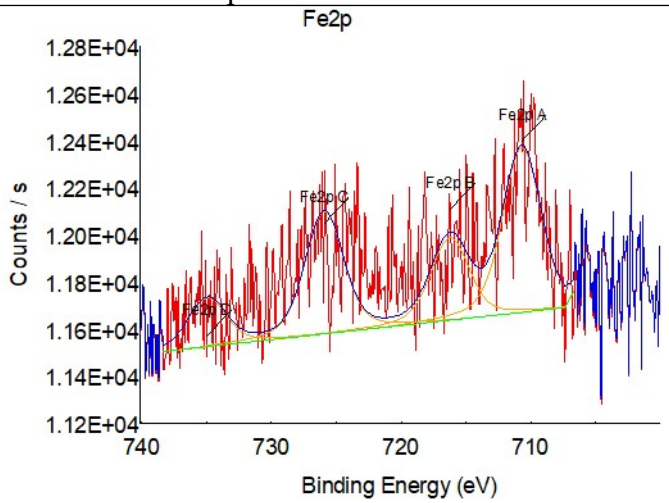

Fe2p GFCFFeGMAPP

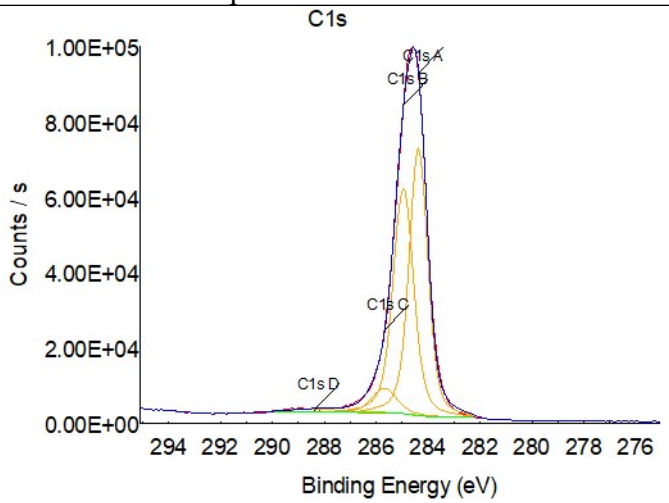

C1s GMAPP

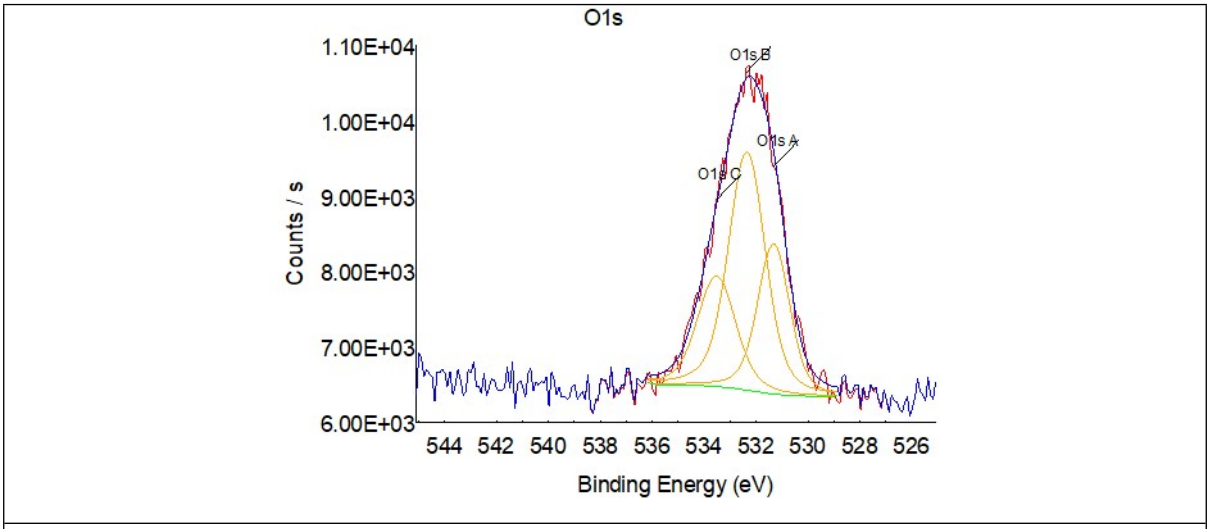

O1s GMAPP

Figure S3. XPS fitting curve of PP composites

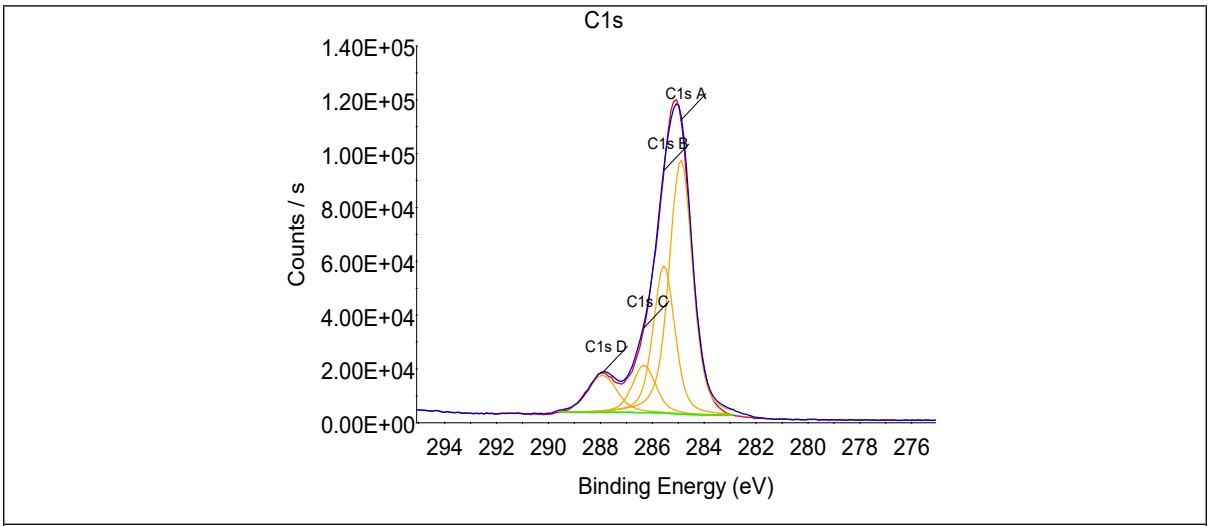

C1s of NFCoT

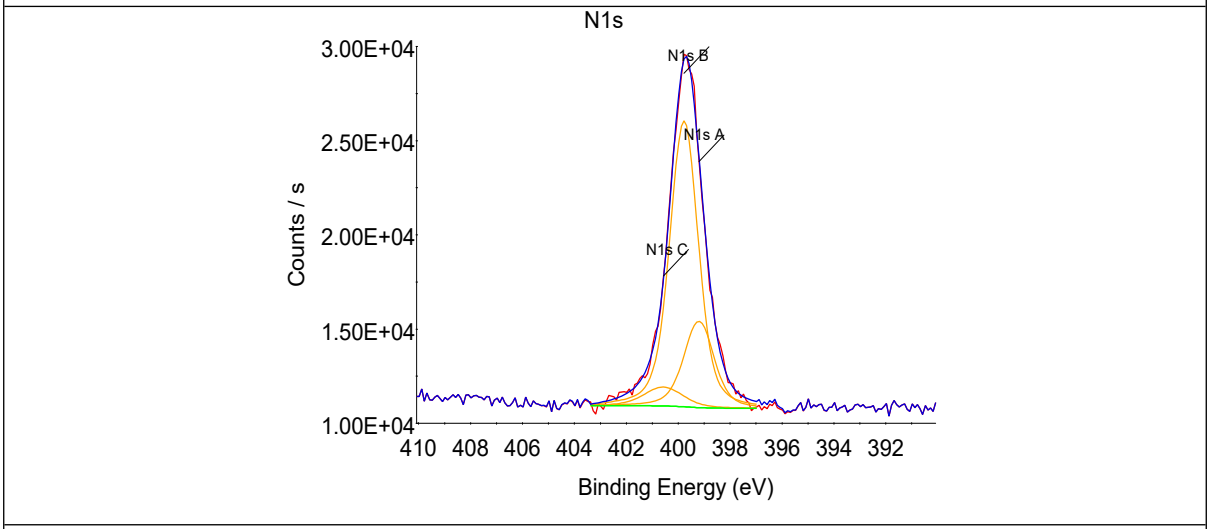

N1s of NFCoT

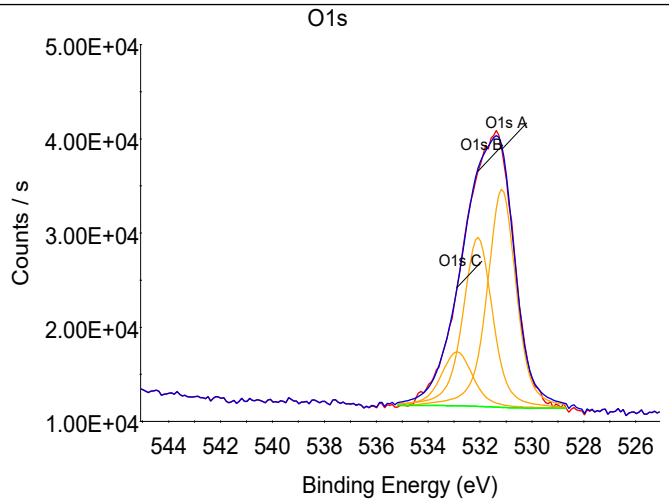

O1s of NFCoT

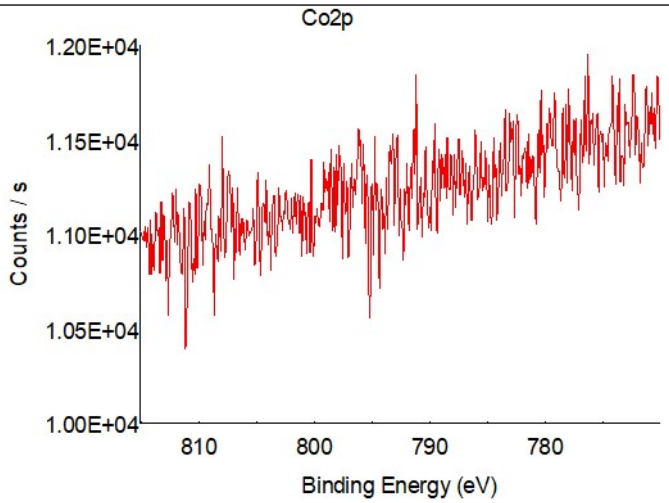

Co2p of NFCoT

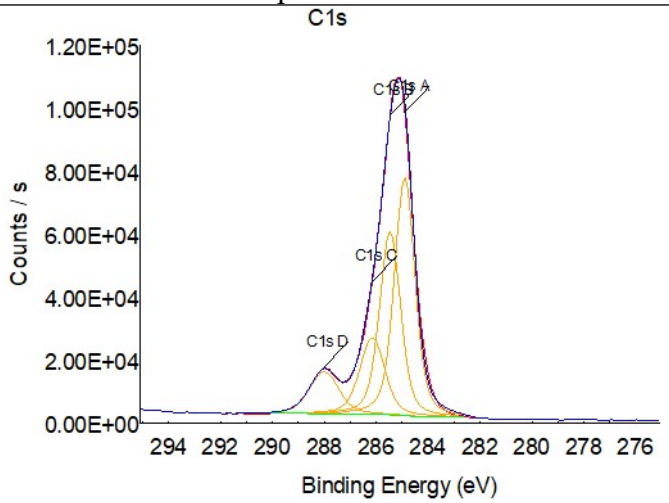

C1s of NFGT

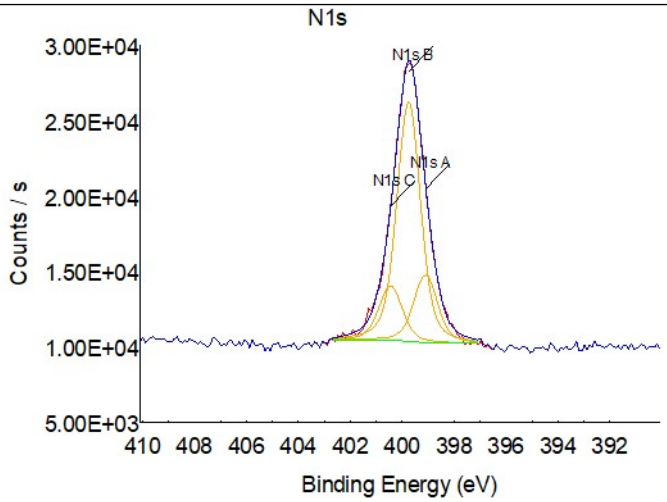

N1s of NFGT

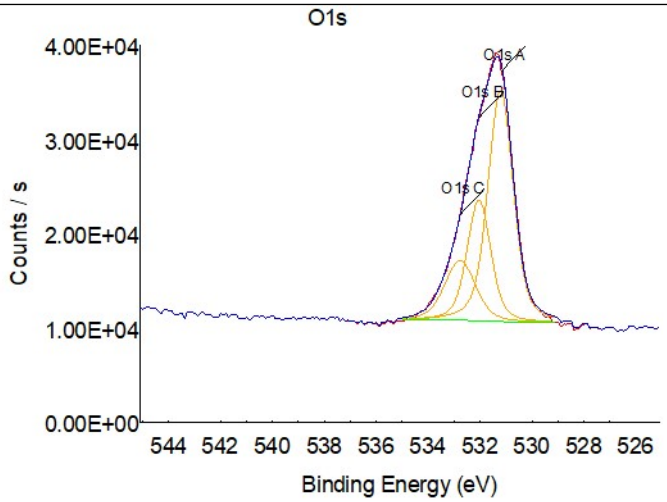

O1s of NFGT

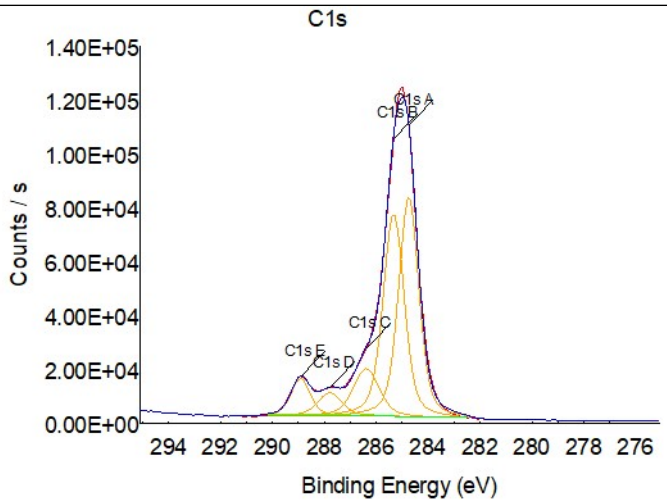

C1s of NGT

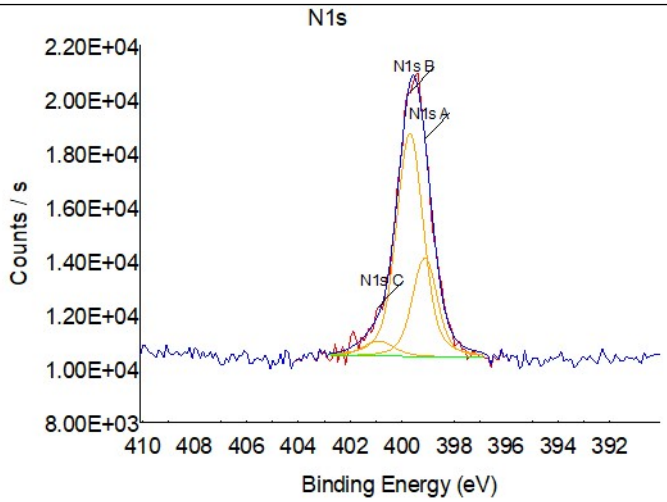

N1s of NGT

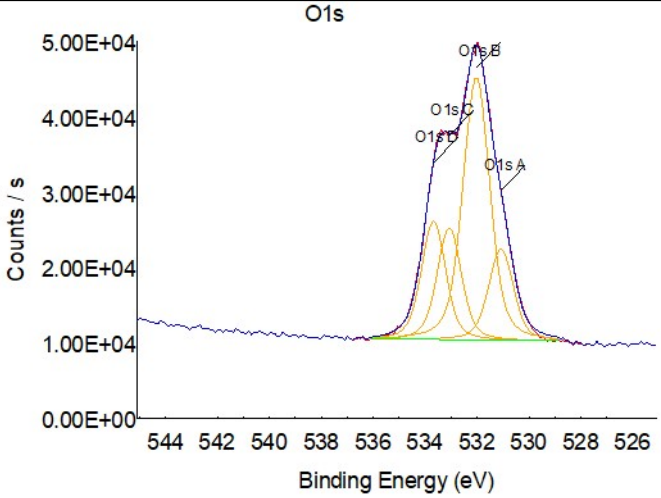

O1s of NGT

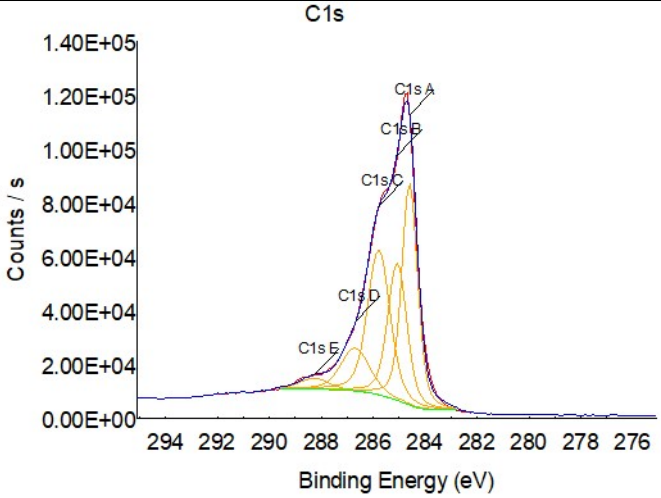

C1s of NGCu

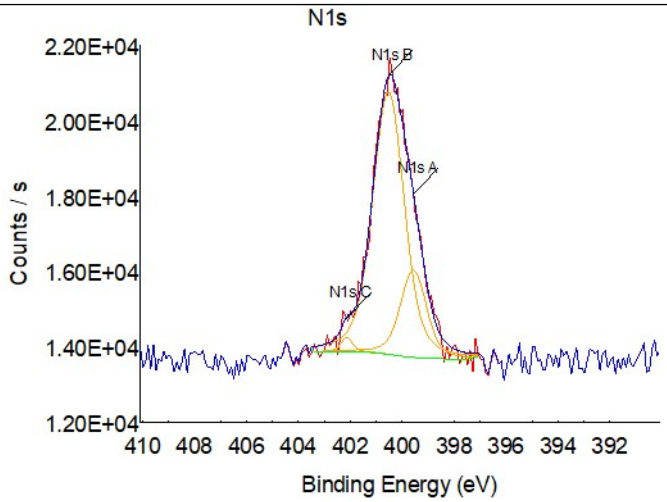

N1s of NGCu

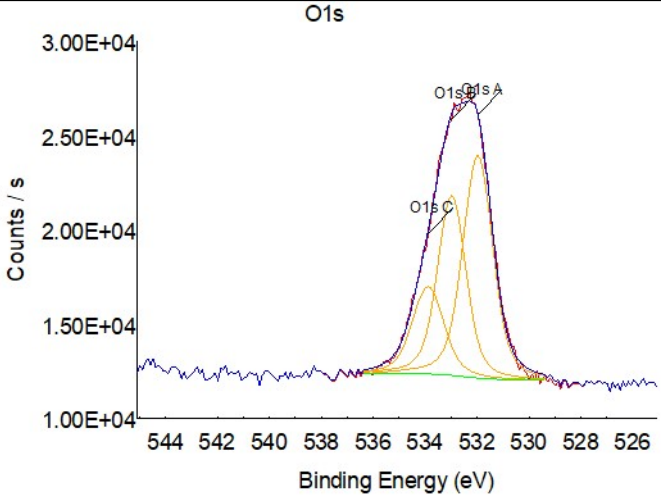

O1s of NGCu

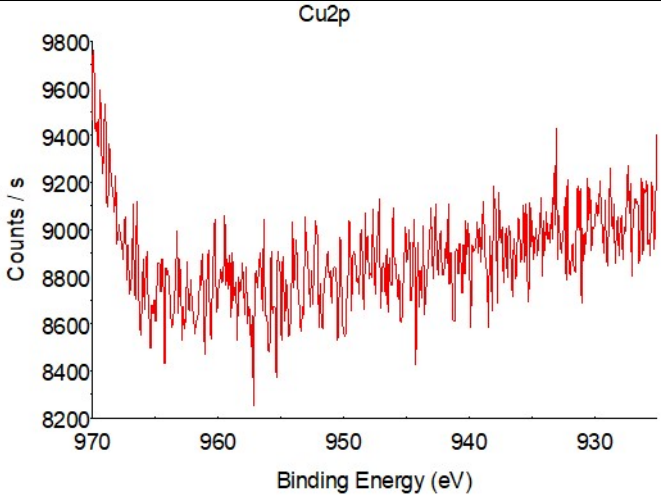

Cu2p of NGCu

Figure S4. XPS fitting curve of nylon-based composite.

EMI shielding of the composites

Figure S5. Polypropylene GGF composite

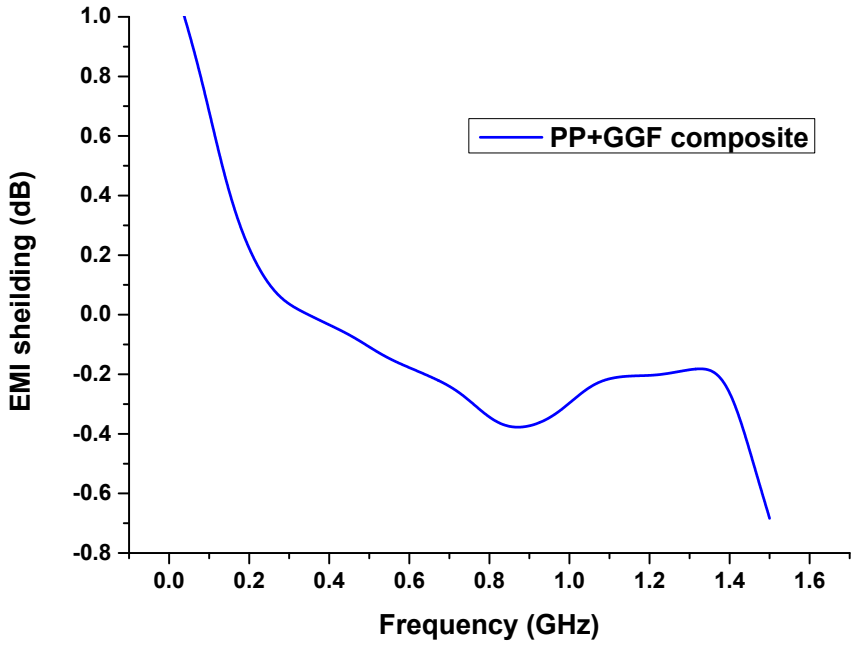

Figure S6. EMI-SE of Polypropylene GGF composite

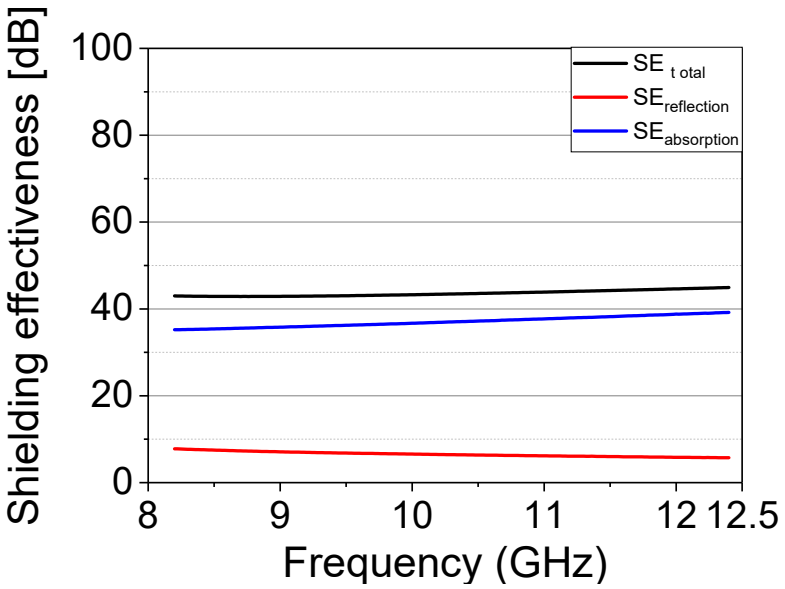

Figure S7. EMI shielding of nylon composite without fillers

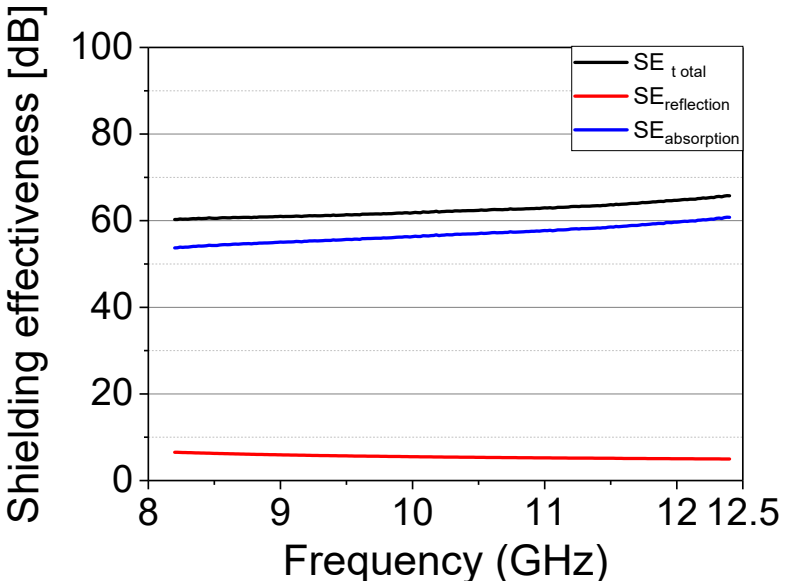

Figure S8. EMI-SE of nylon composite (One time pressed)

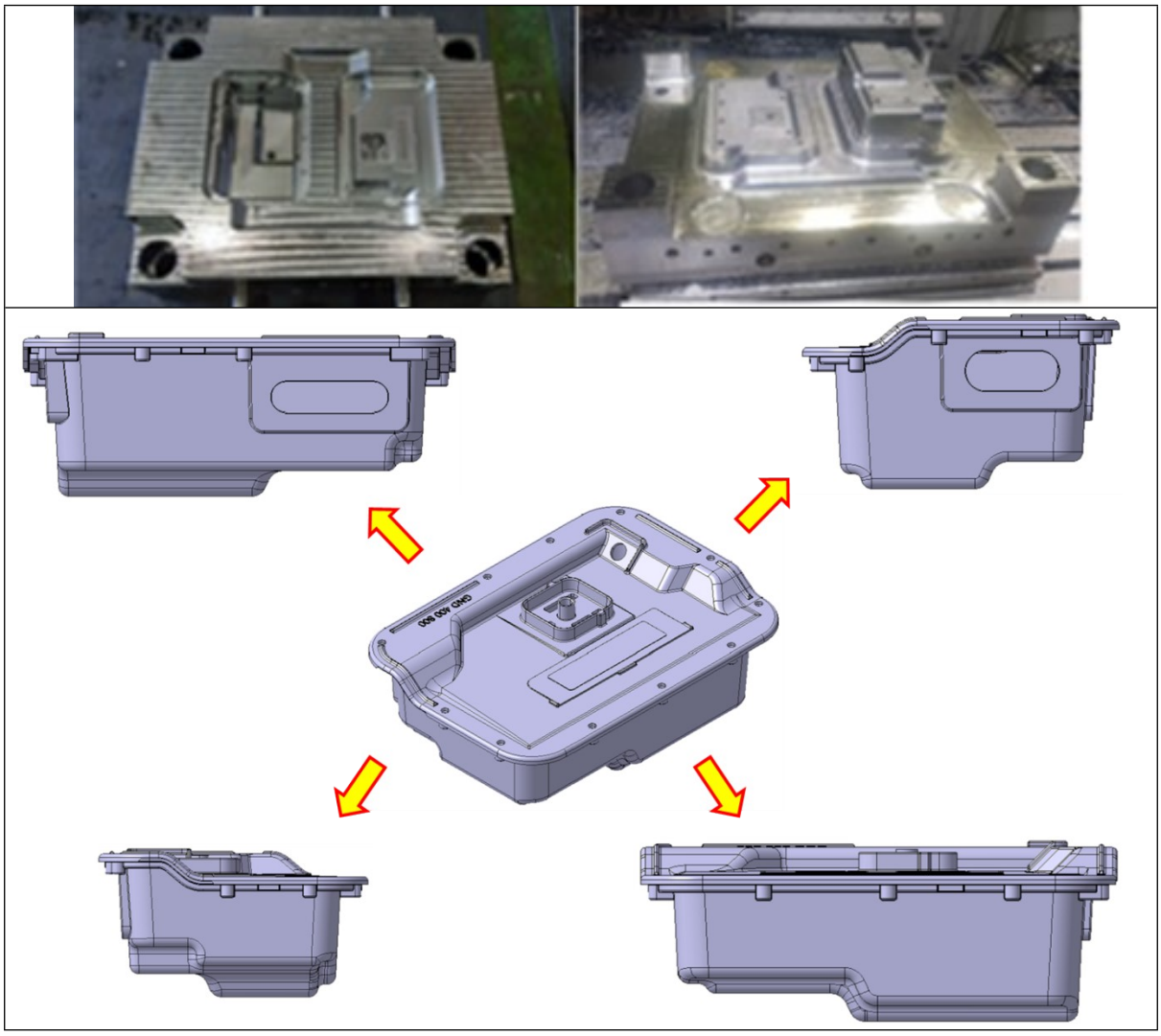

Figure S9. EMI-SE cover for automobile parts.

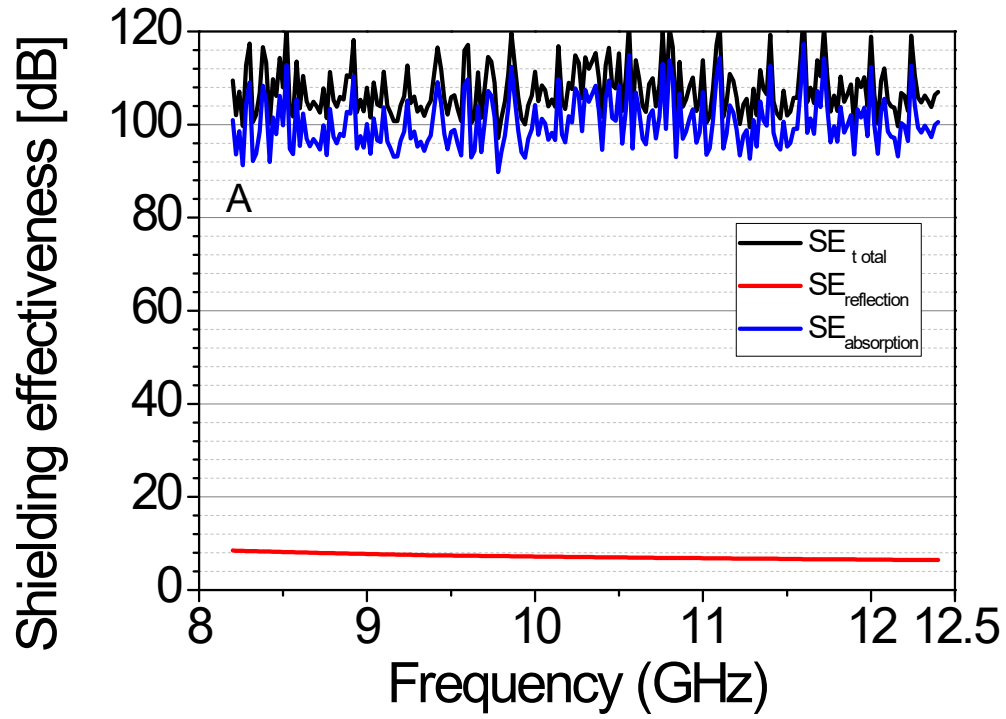
Shielding effectiveness [dB]
120
100
80
60
40
20
0
A
SE t otal
SE reflection
SE absorption
8
9
10
11
12
12.5
Frequency (GHz)

(a)

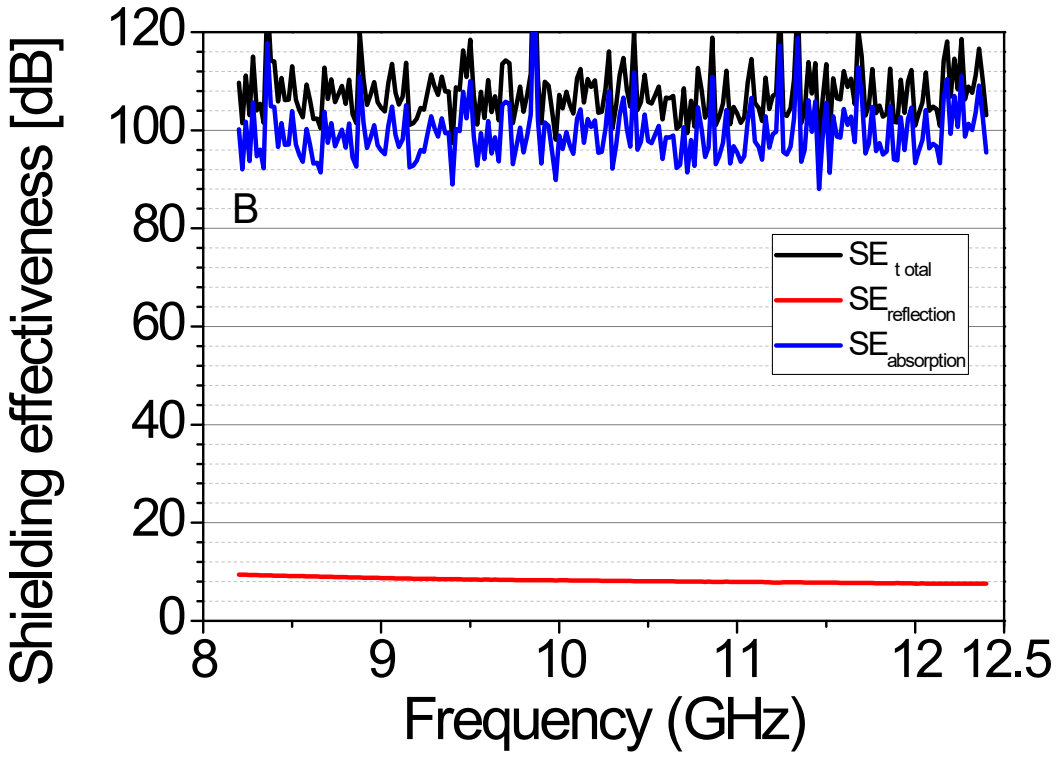
Shielding effectiveness [dB]
120
100
80
60
40
20
0
B
SE t otal
SE reflection
SE absorption
8
9
10
11
12
12.5
Frequency (GHz)

(b)

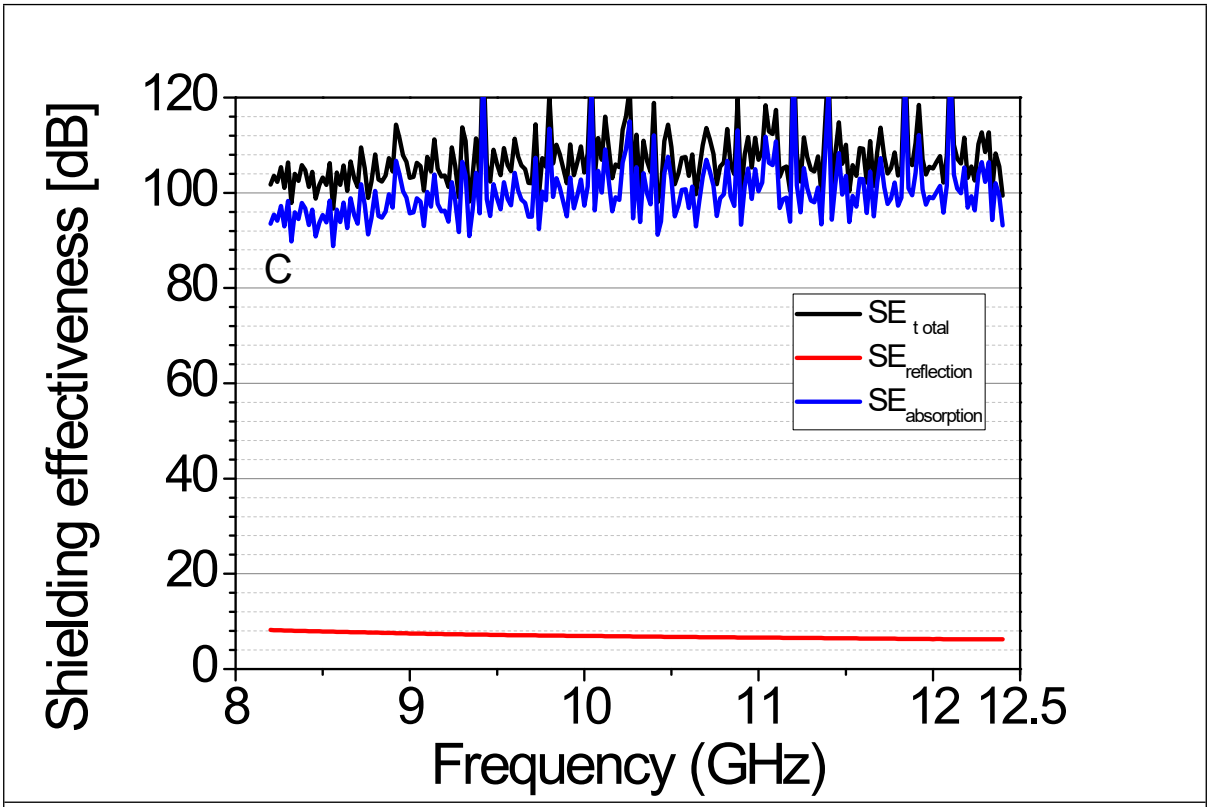

(c)

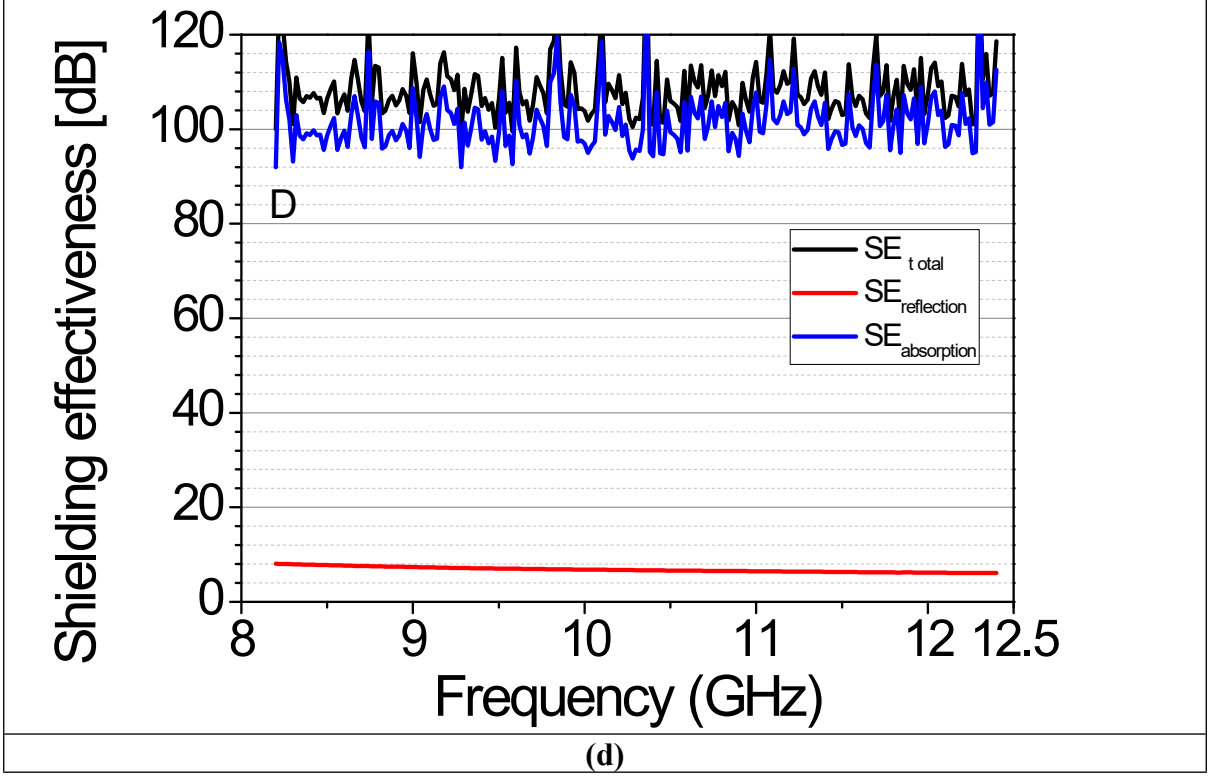

(d)

Figure S10. EMI- SE of composites with 5 mm thickness (a) NFCoT, (b) NFGT, (c) NGT, and (d) NGCu

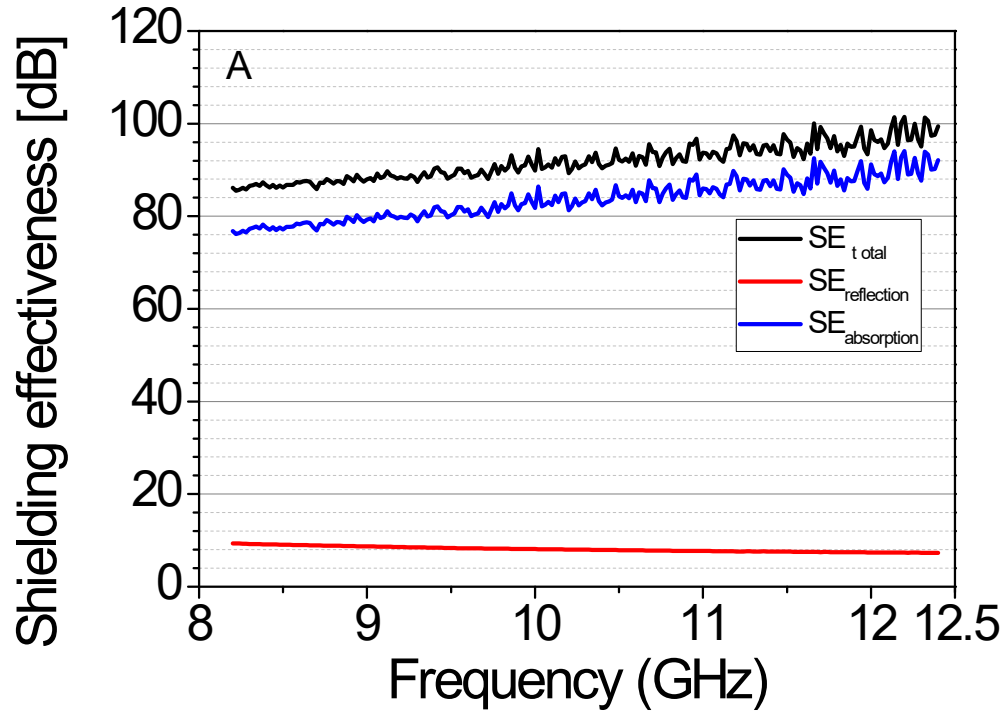
A
Shielding effectiveness [dB]
Frequency (GHz)
SE t otal
SE reflection
SE absorption
0
20
40
60
80
100
120
8
9
10
11
12
12.5

(a)

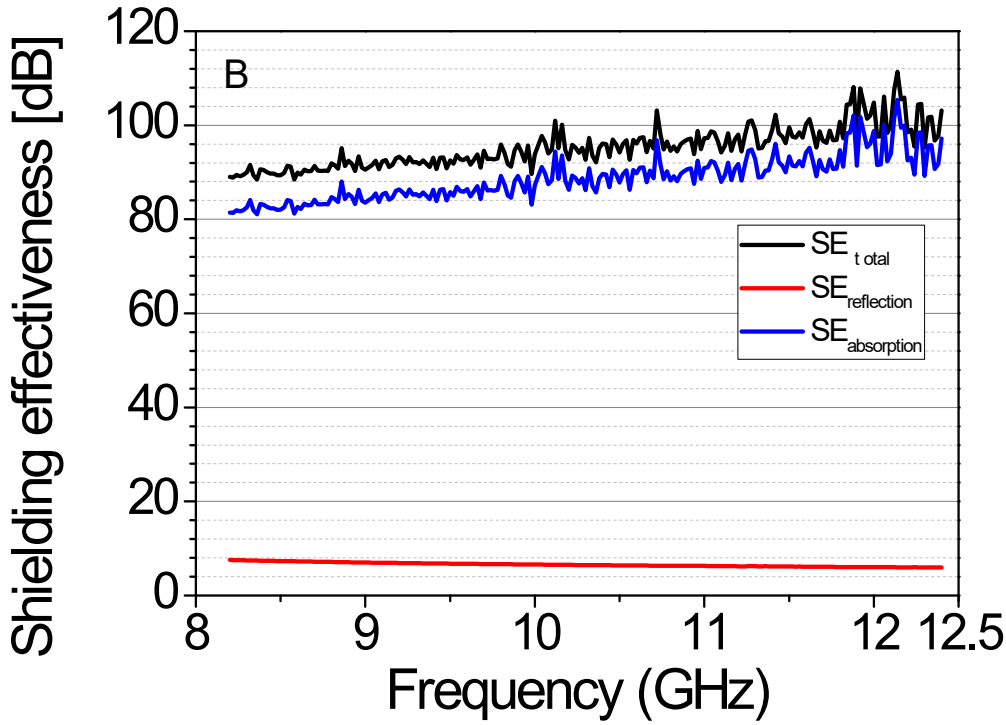
B
Shielding effectiveness [dB]
Frequency (GHz)
SE t otal
SE reflection
SE absorption
0
20
40
60
80
100
120
8
9
10
11
12
12.5

(b)

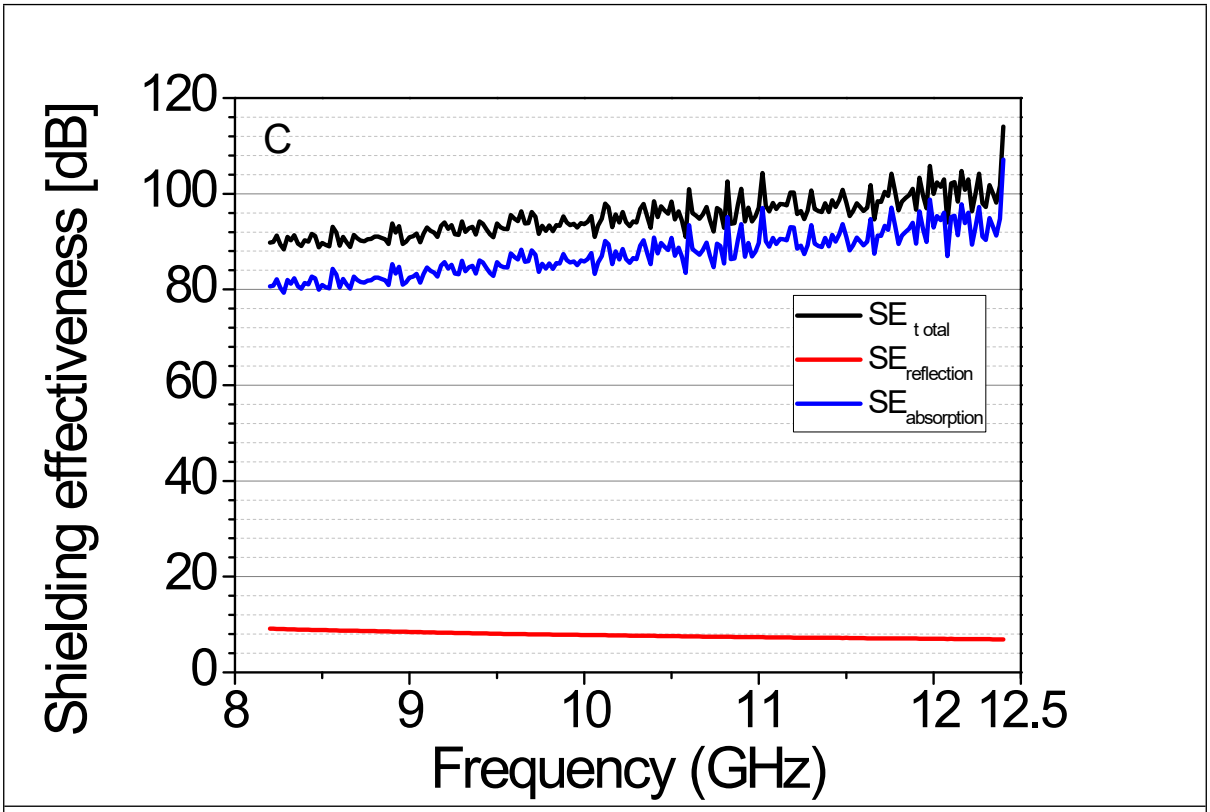

(c)

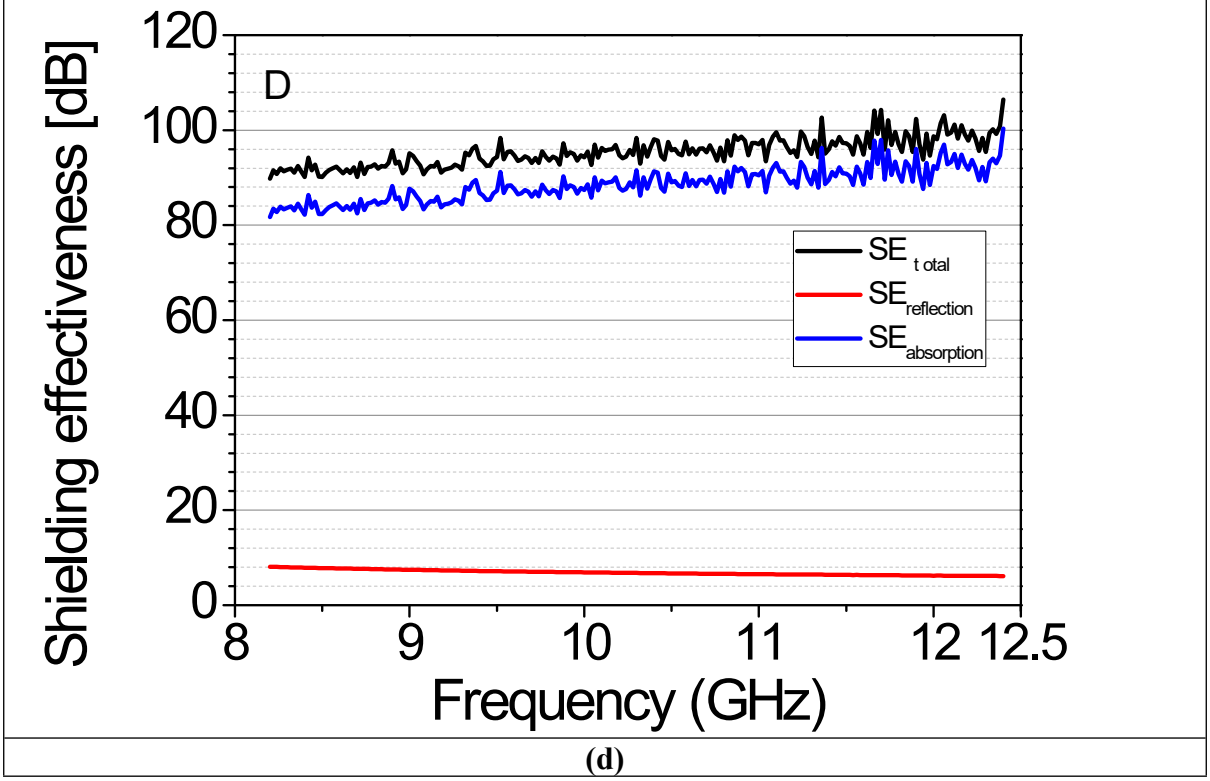

(d)

Figure S11. EMI- SE of composites with 4 mm thickness (a) NFCoT, (b) NFGT, (c) NGT, and (d) NGCu

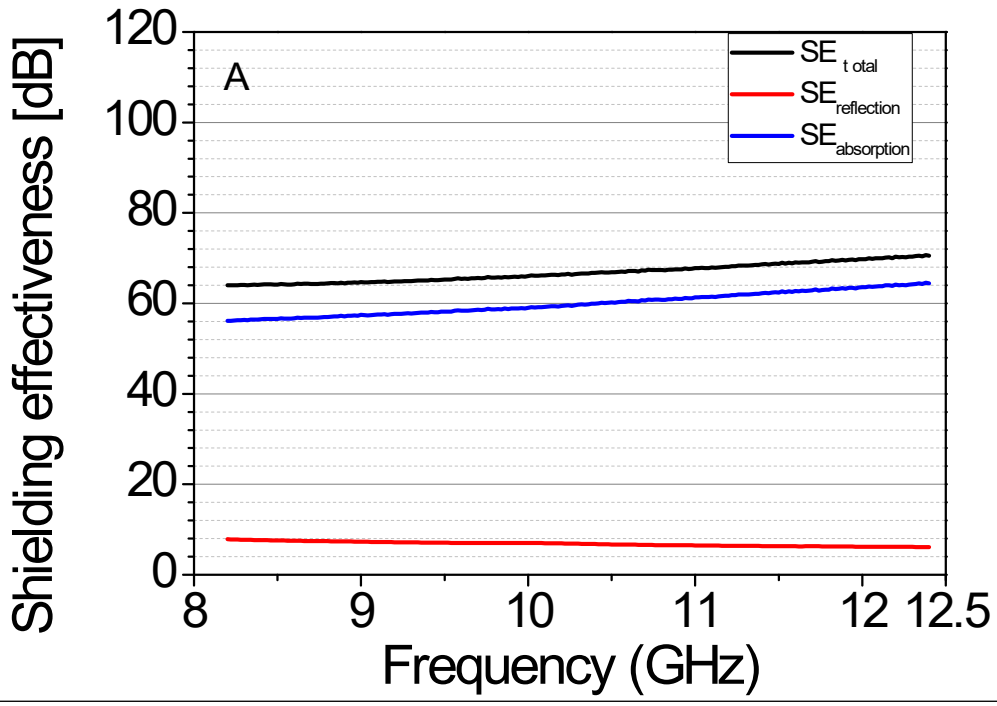
A
SE t otal
SE reflection
SE absorption
Shielding effectiveness [dB]
Frequency (GHz)
0
20
40
60
80
100
120
8
9
10
11
12
12.5

(a)

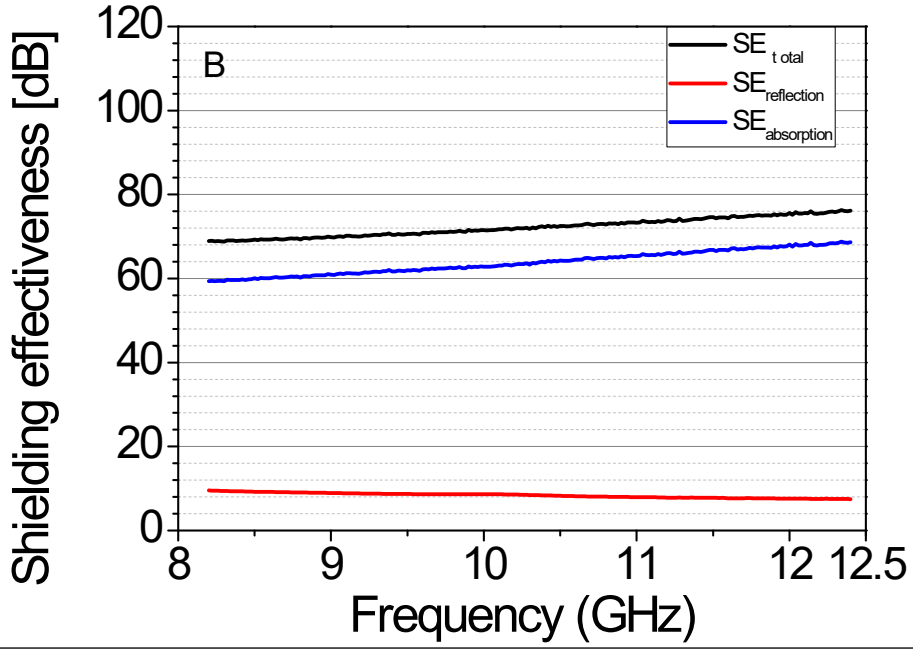
B
SE t otal
SE reflection
SE absorption
Shielding effectiveness [dB]
Frequency (GHz)
0
20
40
60
80
100
120
8
9
10
11
12
12.5

(b)

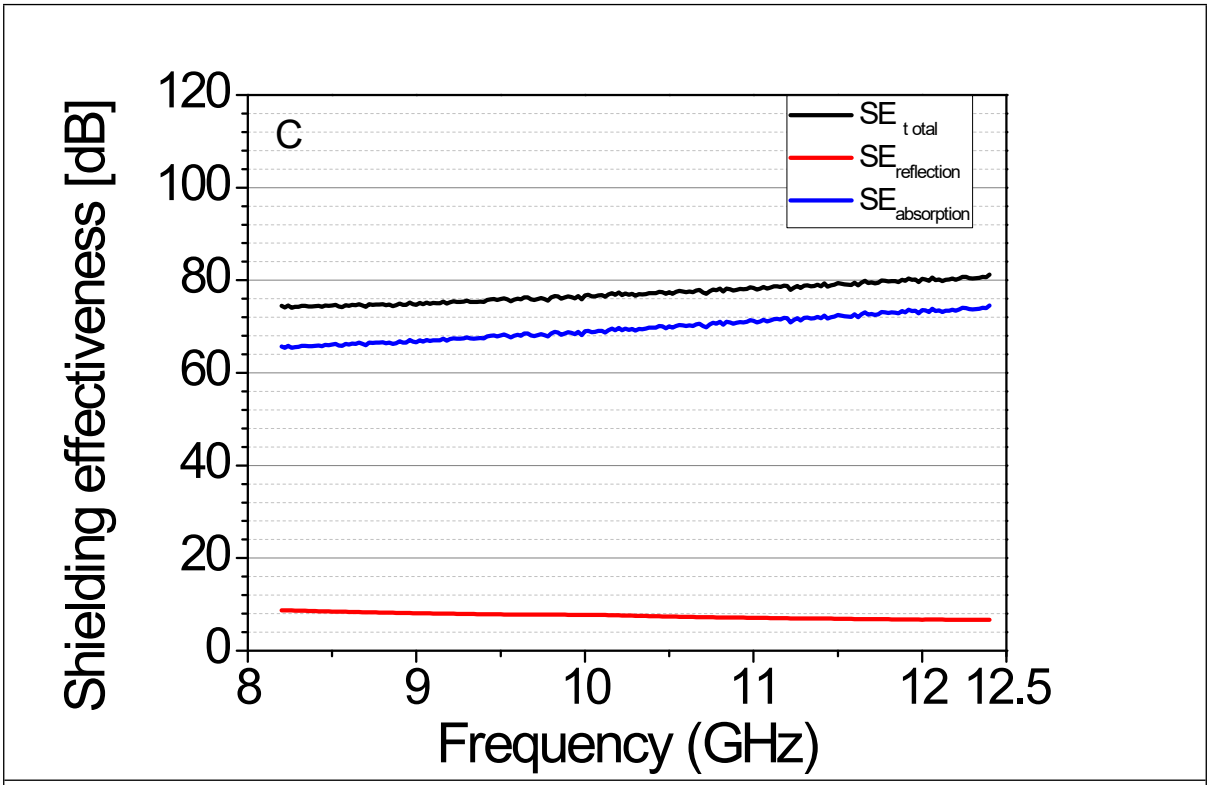

(c)

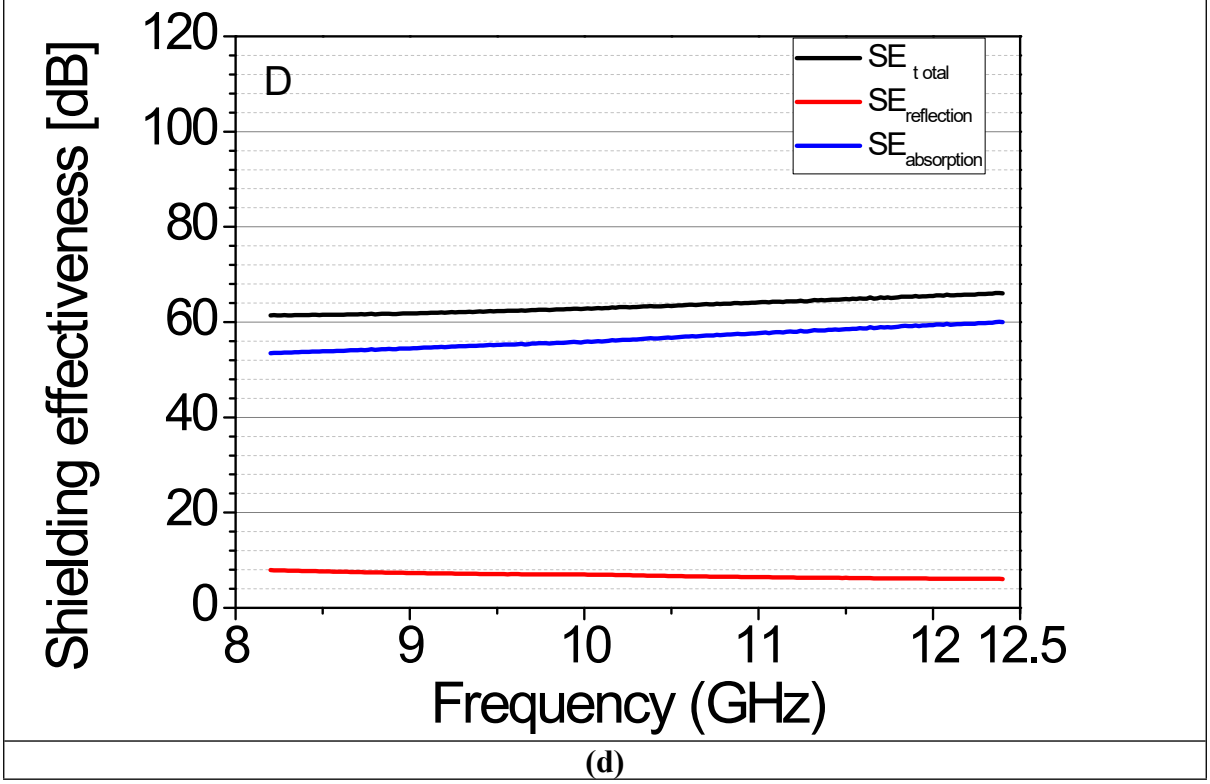

(d)

Figure S12. EMI- SE of composites with 3 mm thickness (a) NFCoT, (b) NFGT, (c) NGT, and (d) NGCu

3. Tables

Table S1. Comparison of total EMI shielding of PP composites (SE_T)

SE_T	GFGMAPP (1)	GFCFGMAPP (2)	GFCFFeGMAPP (3)	GFCFGMAPP+GFCFFeGMAPP (2+3)	GFGMAPP+GFCFGMAPP+GFCFFeGMAPP (1+2+3)
Max	75.18	65.08	72.18	120.11	120.55
Ave	72.75769076	61.89	68.938	101.27	102.97
Mini	71.715	59.99	66.29	91.97	94.53
Efficiency (%)	99.99999697	99.9999689	99.99999395	~100	~100
Thickness (mm)	4.06	4.67	2.56	7.23	11.29

Table S2. Comparison of SE_A of PP composites

SE_A	GFGMAPP (1)	GFCFGMAPP (2)	GFCFFeGMAPP (3)	GFGMAPP+GFCFGMAPP (1+2)	GFGMAPP+GFCFGMAPP+GFCFFeGMAPP (1+2+3)
Max	69.97	62.19	67.39	113.36	113.52
Ave	67.05	58.28	63.95	94.8	96.49
Min	65.10	55.22	61.08	84.59	88.17

Table S3. Comparison of SE_R of PP composites

SE_R	GFGMAPP (1)	GFCFGMAPP (2)	GFCFFeGMAPP (3)	GFGMAPP+GFCFGMAPP (1+2)	GFGMAPP+GFCFGMAPP+GFCFFeGMAPP (1+2+3)
Max	6.68	4.79	5.73	7.38	7.40
Ave	5.71	3.63	4.99	6.47	6.47
Min	5.19	2.88	4.78	5.60	5.59

Total EMI-SE (SE)

Table S4. Comparison of SE_T of Nylon composites

Composites	SE											
	Thickness											
	6 mm			5 mm			4 mm			3 mm		
	max	Ave	Mini	max	Ave	Mini	max	Ave	Mini	max	Ave	Mini
NFCoT	132.9	108.4	99.8	123.9	107.5	97.1	101.4	91.8	85.5	70.7	66.8	63.9
NFGT	132.4	108.9	97.05	139.1	107.7	95.8	111.4	95..3	88.5	76.3	72.2	68.8
NGT	129.4	108.7	98.9	132.6	107.1	96.7	114.1	95.2	88.4	81.2	77.2	74.1
NGCu	138.8	108.2	97.9	136	108.4	99.1	106.5	95.4	89.8	66.1	63.4	61.4

Table S5. Comparison of SE_R of Nylon composites

Composites	SE_R											
	Thickness											
	6 mm			5 mm			4 mm			3 mm		
	max	Ave	Mini	max	Ave	Mini	max	Ave	Mini	max	Ave	Mini
NFCoT	9.7	8.4	7.5	9.5	7.2	6.4	9.4	8.1	7.3	7.9	6.8	6.1
NFGT	9.7	8.3	7.6	9.4	8.3	7.6	7.6	6.6	5.9	9.5	8.4	7.5
NGT	7.9	6.8	6.1	8.2	6.9	6.2	9.1	7.8	6.9	8.8	7.5	6.7
NGCu	9.9	7.7	6.9	8.1	6.82	6.1	8.1	6.9	6.1	7.9	6.8	6.1

Table S6. Comparison of SE_A of Nylon composites

Composites	SE_A											
	Thickness											
	6 mm			5 mm			4 mm			3 mm		
	max	Ave	Mini	max	Ave	Mini	max	Ave	Mini	max	Ave	Mini
NFCoT	123.5	99.9	91.3	117.3	100.3	89.8	94.1	83.7	76.2	64.6	59.9	56.2
NFGT	124.8	100.6	87.9	130.8	99.4	88.0	105.4	88.7	81.1	68.8	63.8	59.4
NGT	122.5	101.9	92.4	126.1	100.2	88.8	107.1	87.4	79.4	74.5	69.6	65.4
NGCu	131.6	100.5	90.9	129.3	101.5	91.9	100.3	88.5	81.7	60	56.6	53.5

Table S7. Comparison of EMI shielding of the composites

No	Composition	Filler (%)	Thickness (mm)	EMI-SE (dB)	SE/d (dB/mm)	Ref.
1	Segregated Graphene/ Polypropylene	10	0.9 mm	19.3	21.44	1
2	Polypropylene/conductive fiber	20	2 mm	43	21.50	2
3	Carbon black/polypropylene (PP)	10	2.8 mm	42.7	15.25	3
4	RGO/PP	1.83	0.7 mm	29.3	41.86	4
5	Carbon fiber/PP	10	3.2 mm	25	7.81	5
6	$Ti_3C_2T_x$/PP	2.12	1.93 mm	66	34.19	5
7	$Ti_3C_2T_x$/PP	1.78	1.93 mm	55	28.50	5
8	Ti_3C_2Tx/wax	90	1 mm	32	32	5
9	CNT/PU	20	2 mm	17	8.5	5
10	Segregated CNT/PP	3.5	2 mm	32	16	6
11	Epoxy Cu-nanowires/ GN aerogel	7.2	2 mm	47	23.5	7
12	GN foam/acrylonitrile butadiene styrene	50	1.6 mm	42.4	26.5	8
13	poly(ε-caprolactone)/MWCNT	50	2.4 mm	44	18.34	9
14	Recyclable conductive epoxy/CNT	1	1.8 mm	22	12.23	10
15	PP/carbon black foam	30	60 mm	41	0.68	11
16	Microwires-graphene/Silicone elastomer (M/G/S)	0.0193	2 mm	18	9	12
17	Bucky-paper/polyethylene	38	0.025 mm	20	800	12
18	PP/carbon fiber	20	2 mm	-32.92	-16.46	13
19	PAN@SiO_2-4wt%Ag-30min	4	0.05 mm	22.68	533.6	14
20	PAN@SiO_2-4wt%Ag-12h-PFDT film	4	0.05	81	1620	14
21	Ni@nylon mesh/PP	3.07	2.5 mm	50.6	20.24	15
22	Porous POM/MWCNT	10	2 mm	58.5	29.3	16
23	Water-based Conductive Ink	80	0.01 mm	74.5	7450	17
24	GFGMAPP(1)	13	4.06 mm	75.18	18.52	This work
25	GFCFGMAPP (2)	13	4.67 mm	65.08	13.94	
26	GFCFFeGMAPP (3)	13	2.56 mm	72.18	28.20	
27	1+2	13	7.23	120.11	16.61	
28	1+2+3	13	11.29	120.55	10.68	
29	NFCoT	13	6 mm	132.9	22.15	
30	NFGT	13	6 mm	132.4	22.07	
31	NGT	13	6 mm	129.4	21.57	
32	NGCu	13	6 mm	138.8	23.14	

References

1. Alam, F.E., Yu, J., Shen, D., Dai, W., Li, H., Zeng, X., Yao, Y., Du, S., Jiang, N. and Lin, C.T., 2017. Highly conductive 3D segregated graphene architecture in polypropylene composite with efficient EMI shielding. Polymers, 9(12), p.662.
2. Lee PC, Kim BR, Jeoung SK, Kim YK. Electromagnetic interference shielding effectiveness of polypropylene/conducting fiber composites. InAIP Conference Proceedings 2016 Mar 9 (Vol. 1713, No. 1, p. 120015). AIP Publishing LLC.
3. Al-Saleh, M.H. and Sundararaj, U., 2012. X-band EMI shielding mechanisms and shielding effectiveness of high structure carbon black/polypropylene composites. Journal of Physics D: Applied Physics, 46(3), p.035304.
4. Sun, T., Luo, W., Luo, Y., Wang, Y., Zhou, S., Liang, M., Chen, Y. and Zou, H., 2020. Self-Reinforced Polypropylene/Graphene Composite with Segregated Structures To Achieve Balanced Electrical and Mechanical Properties. Industrial & Engineering Chemistry Research, 59(24), pp.11206-11218.
5. Xu, M.K., Liu, J., Zhang, H.B., Zhang, Y., Wu, X., Deng, Z. and Yu, Z.Z., 2021. Electrically Conductive Ti3C2T x MXene/Polypropylene Nanocomposites with an Ultralow Percolation Threshold for Efficient Electromagnetic Interference Shielding. Industrial & Engineering Chemistry Research, 60(11), pp.4342-4350.
6. Zhang, Y.P., Zhou, C.G., Sun, W.J., Wang, T., Jia, L.C., Yan, D.X. and Li, Z.M., 2020. Injection molding of segregated carbon nanotube/polypropylene composite with enhanced electromagnetic interference shielding and mechanical performance. Composites Science and Technology, 197, p.108253.
7. Yang, X., Fan, S., Li, Y., Guo, Y., Li, Y., Ruan, K., Zhang, S., Zhang, J., Kong, J. and Gu, J., 2020. Synchronously improved electromagnetic interference shielding and thermal conductivity for epoxy nanocomposites by constructing 3D copper nanowires/thermally annealed graphene aerogel framework. Composites Part A: Applied Science and Manufacturing, 128, p.105670.
8. Wang, L., Wu, Y., Wang, Y., Li, H., Jiang, N. and Niu, K., 2020. Laterally compressed graphene foam/acrylonitrile butadiene styrene composites for electromagnetic interference shielding. Composites Part A: Applied Science and Manufacturing, 133, p.105887.
9. Tang, X.H., Li, J., Tan, Y.J., Cai, J.H., Liu, J.H. and Wang, M., 2020. Achieve high performance microwave shielding in poly (ε-caprolactone)/multi-wall carbon nanotube composites via balancing absorption in conductive domains and multiple scattering at interfaces. Applied Surface Science, 508, p.145178.
10. Yuan, D., Guo, H., Ke, K. and Manas-Zloczower, I., 2020. Recyclable conductive epoxy composites with segregated filler network structure for EMI shielding and strain sensing. Composites Part A: Applied Science and Manufacturing, 132, p.105837.
11. Li, Y., Lan, X., Wu, F., Liu, J., Huang, P., Chong, Y., Luo, H., Shen, B. and Zheng, W., 2020. Steam-chest molding of polypropylene/carbon black composite foams as broadband EMI shields with high absorptivity. Composites Communications, 22,

p.100508.

12. Xu, Y.L., Uddin, A., Estevez, D., Luo, Y., Peng, H.X. and Qin, F.X., 2020. Lightweight microwire/graphene/silicone rubber composites for efficient electromagnetic interference shielding and low microwave reflectivity. Composites Science and Technology, 189, p.108022.

13. Kaushal, A. and Singh, V., 2020. Development of lightweight polypropylene/carbon fiber composites for its application in shielding of electromagnetic interference in X-band. Journal of Materials Science: Materials in Electronics, 31(17), pp.14088-14100.

14. Li, T.T., Wang, Y., Peng, H.K., Zhang, X., Shiu, B.C., Lin, J.H. and Lou, C.W., 2020. Lightweight, flexible and superhydrophobic composite nanofiber films inspired by nacre for highly electromagnetic interference shielding. Composites Part A: Applied Science and Manufacturing, 128, p.105685.

15. Li, S., Xu, Z., Dong, Y., Liu, D. and Sui, G., 2020. Ni@ nylon mesh/PP composites with a novel tree-ring structure for enhancing electromagnetic shielding. Composites Part A: Applied Science and Manufacturing, 131, p.105798.

16. Li, J., Chen, J.L., Tang, X.H., Cai, J.H., Liu, J.H. and Wang, M., 2020. Constructing nanopores in poly (oxymethylene)/multi-wall carbon nanotube nanocomposites via poly (l-lactide) assisting for improving electromagnetic interference shielding. Journal of colloid and interface science, 565, pp.536-545.

17. Jia, L.C., Zhou, C.G., Sun, W.J., Xu, L., Yan, D.X. and Li, Z.M., 2020. Water-based conductive ink for highly efficient electromagnetic interference shielding coating. Chemical Engineering Journal, 384, p.123368.